Applied Physics A (2020) 126:671
https://doi.org/10.1007/s00339-020-03851-5

Applied Physics A
Materials Science & Processing

Study of boron diffusion for p + emitter of large area N-type TOPCon silicon solar cells

Ying Zhou[1,2,4] · Ke Tao[2,4] · Aimin Liu[1] · Rui Jia[2,4] · Shuai Jiang[2,4] · Jianhui Bao[1,2] · Sanchuan Yang[3] · Yujia Cao[3] · Hui Qu[3]

Received: 2 March 2020 / Accepted: 24 July 2020

Abstract
Boron doped emitters prepared by thermal diffusion using boron trichloride (BCl_3) have been adopted in N-type Tunnel Oxide Passivated Contact (TOPCon) silicon solar cells. In order to establish a proper diffusion process of p + emitter that matches to TOPCon solar cells fabrication, the influence of diffusion pressure, pre-deposition O_2 flow rate and drive-in O_2 flow rate on the doping profiles, sheet resistance, BSG thickness as well as the sheet resistance uniformity are carefully investigated. In addition, the impact of BSG thickness on the surface morphology and optical properties of the TOPCon cells are studied. The experimental results indicate that good uniformity of p + emitter can be obtained at low pressure (300 mbar) with acceptable sheet resistance. In addition, a p + emitter with thick BSG (> 50 nm) layer is very necessary, which can effectively protect the underneath emitter during the removal process of the wrap-around poly-Si. Finally, high efficiency over 22% is obtained for 244.32 cm^2 n-type TOPCon solar cells based on the boron diffused emitter with the sheet resistance 70–90 ohm/sq., BSG thickness ~ 100 nm.

Keywords Tunnel oxide passivated contact · Boron diffusion · Boron trichloride (BCl_3) · Vacuum

1 Introduction

Recently, N-type tunnel oxide passivated contact solar cell has attracted much interest thanks to the excellent passivation and effective carrier transport [1]. Various methods [2–4] have been used to form the P-doped polycrystalline silicon layer, especially, intrinsic poly-Si by LPCVD combined with $POCl_3$ diffusion has been successfully applied in mass production of TOPCon solar cells [5]. However, during the deposition of poly-Si, wrap-around takes place, which leads to poor performance of solar cells. It's necessary to remove the wrap-around poly-Si thin film on the front surface of substrate [6]. Thus, in order to protect the optical properties and metal contact of the front surface from other progress (poly-Si wrap-around removing and $POCl_3$ diffusion), a high quality p + emitter with a suitable sheet resistance and a thick BSG is necessary.

Boron doping has been used for p + emitter formation in N type silicon solar cells, and on the industrial, direct thermal diffusion of boron trichloride (BCl_3) or boron tribromide (BBr_3) is usually used as doping sources [7–9]. And it has been found that the Cl_2 formed during the thermal diffusion of BCl_3 can increase the electrical stability of oxide [10]. The p + emitter formation using BCl_3 can be described by two processes: pre-deposition process and drive-in process. During the pre-deposition process, Borosilicate Glass (BSG) comprised by Silicon Dioxide (SiO_2) and boron oxide is formed [11] and during the drive-in process, the atomic boron diffused into silicon structure rapidly with the assist of high temperature. It is well know that the oxidation enhanced diffusion (OED) is performed in boron diffusion during the thermal oxidation [12, 13] and has been explained by the supersaturation of lattice point defects during oxidation. It

✉ Ke Tao
taoke@ime.ac.cn

✉ Aimin Liu
aiminl@dlut.edu.cn

✉ Rui Jia
imesolar@126.com

[1] School of Microelectronics, Dalian University of Technology, Dalian, People's Republic of China

[2] Institute of Microelectronics, Chinese Academy of Science, Beijing 100029, China

[3] Shunfeng Photovoltaic Technology, JiangSu, People's Republic of China

[4] University of Chinese Academy of Sciences, Beijing 100049, China

Published online: 05 August 2020

has observed that, the diffusion coefficient of boron can be affected by diffusion temperature, diffusion time, substrate orientation, substrate doping concentration and the oxidation ambient [14–16] and the diffusion enhancement ratio increases as the oxidation rate increases [17]. Beside, as an important parameter, the oxidation ambient can also affect the growth of BSG, which can be a protect mask in solar cell fabrication process.

This paper focuses on the boron diffusion behavior based on the O_2 flow rate in industrial TOPCon solar cells fabrication. The doping profiles, like sheet resistance, sheet resistance uniformity and BSG thickness has been investigated in detail as a function of pre-deposition O_2 flow rate and drive-in O_2 flow rate, respectively. Besides, the influence of BSG thickness on TOPCon cell performance has also been studied.

2 Experimental

The samples are fabricated on textured 0.5–1.0 Ω.cm n-type Czochralski (Cz) < 100 > Si wafers (244.32 cm^2). The boron diffusion process is carried out after the standard RCA cleaning [18] and texture in an industrial-scale quartz tube furnace(SEMCO Lydop™) working at 780 ℃–1000 ℃. In order to reduce the effect of the wafer number and position to the experiment, about 200 wafers are used in every B diffusion process with about 10 samples placed in middle of the boat as shown in Fig. 1c. The profile of the diffusion in this work is described by Fig. 1a and three process steps are carried out: pre-deposition process, drive-in process and cool down process. The pre-deposition process of investigated diffusions is performed 50 min between 860 and 900 ℃ and the drive-in process is performed 60 min between 960 and 1000 ℃. The BCl_3 flow rate used in pre-deposition process is 100–175 sccm. The O_2 flow rate in pre-deposition step and drive-in step with different vacuum conditions are studied and the overview of O_2 flow rate for each experiment is shown in Table 1. During the pre-deposition O_2 flow

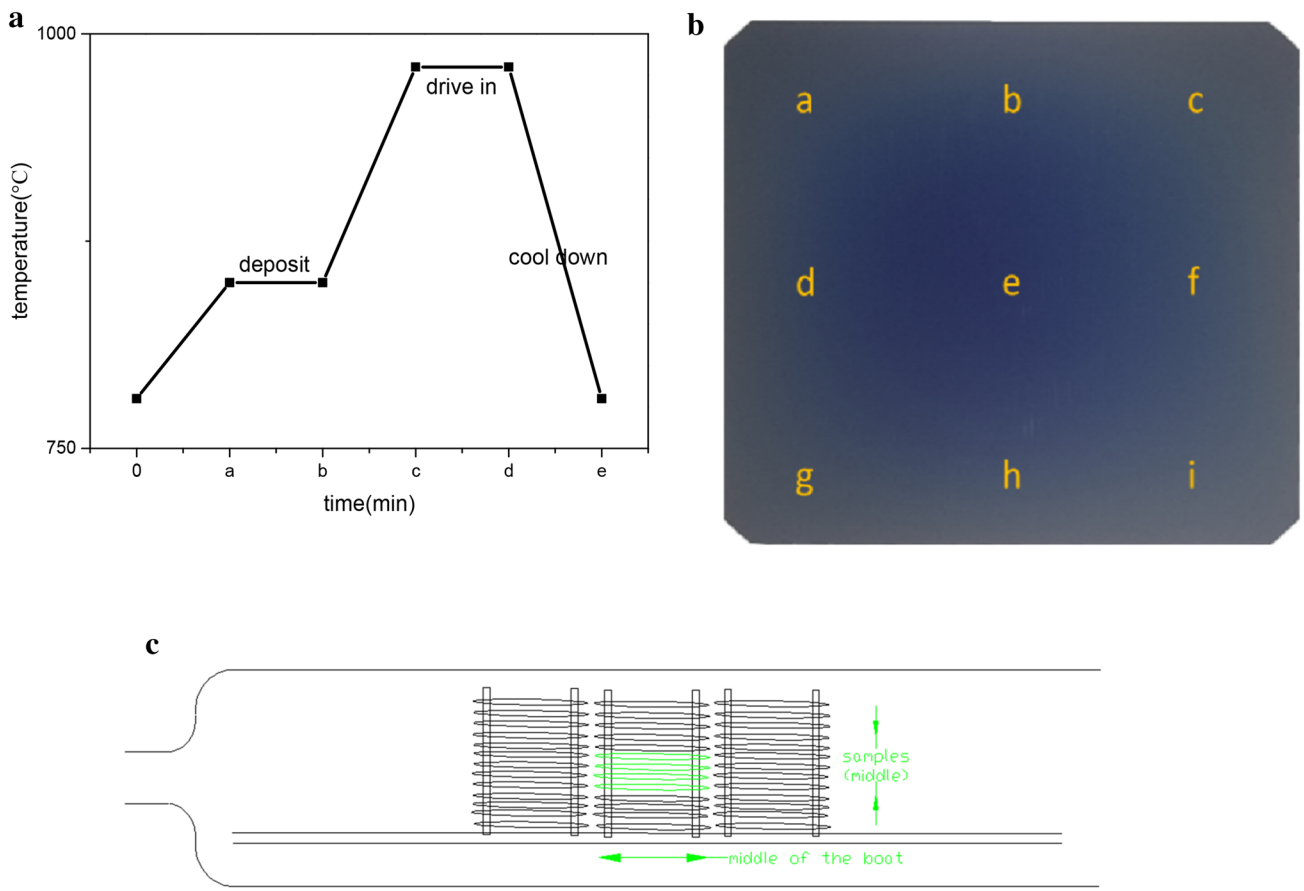

Fig. 1 BCl_3 boron diffusion process **a**. The profile of the diffusion **b**. Location of measurement taken on samples. **c** Industrial diffusion furnace, including sample position

Table 1 Overview of O_2 flow rate for experimental series

Section	Pre-deposition O_2 flow rate (sccm)	Drive-in O_2 flow rate (sccm)	Cool down O_2 flow rate (sccm)
3.1	50	3000	500–1000
	100		
	200		
	300		
3.2	100	0	
		1000	
		2000	
		3000	

rate experiment (Sect. 3.1), the pre-deposition O_2 flow rate various from 50 to 300 sccm while the drive-in O_2 flow rate always be 3000 sccm; during the drive-in O_2 flow rate experiment (Sect. 3.2), the drive-in O_2 flow rate various from 0 to 3000 sccm while the pre-deposition O_2 flow rate is kept at 100 sccm.

Figure 2a shows the schematic drawing of solar cell structure, which features a boron diffused emitter at the front side and tunnel oxide/poly-crystalline silicon passivated contact at the rear side. Figure 2b shows the fabrication process of TOPCon solar cells: after boron diffusion, a single side etching process is performed to remove the boron diffused layer at the rear side of silicon wafers. Then, an ultra-thin tunnel oxide layer ~ 1.5 nm and 100 nm phosphorus-doped polycrystalline silicon layer are deposited successively via LPCVD system. Thereafter, a N_2 annealing is carried out in an inert atmosphere at 850 ℃ to facilitate good passivation quality and dopant activation. After wrap-around poly-Si removed, 4 nm Al_2O_3/80 ~ 90 nm SiN_x and SiN_x are deposited on the front side and back side, respectively. Finally, screen printing and co-firing are performed to form metal contacts.

To measure the sheet resistance, four-point probe (4PP, RG-200PV) is used and 9 points distribution on wafers (as shown in Fig. 1b) are tested to estimate the uniformity of the diffusion, and the corresponding average values are shown in this paper. For the investigation of surface doping concentration and emitter depth profile, electrochemical capacitance voltage (ECV) profiling is used after the BSG layer etched out by a solution composed of hydrofluoric acid and DI water, and all the ECV are measured at the center of the samples. The BSG thickness is measured by scanning electron microscope (SEM) and the surface morphology is measured by optical microscope. External quantum efficiency (EQE) is measured by IPCE of solar cells measurement system (Sofn,7-SCSpec,China), and the electrical performance of solar cells is characterized by a current–voltage (I-V) measurement system (under AM1.5G, R.T.).

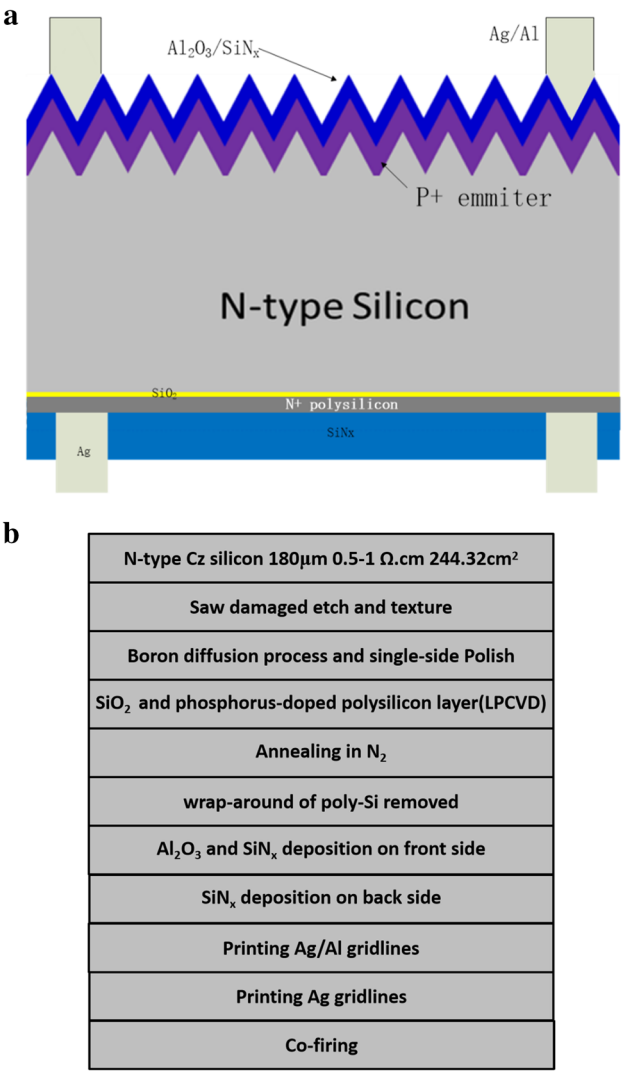

Fig. 2 **a** The schematic drawing of solar cell structure with tunnel oxide/n + poly-crystalline silicon passivated rear contact. **b** the process sequence for the fabrication of TOPCon cells

3 Results and discussion

3.1 O_2 flow rate and diffusion pressure during pre-deposition stage

Figure 3 shows the sheet resistance and ECV profile as a function of pre-deposition O_2 flow rate in various vacuum conditions. Similar tendency is observed for samples prepared at different diffusion pressures (300 mbar, 400 mbar and 500 mbar, respectively), that the sheet resistance decreases gradually with the junction depth increases as the O_2 flow rate increases from 50 to 300sccm. Smaller tendency is also observed from the relationship between the BSG thickness and the O_2 flow rate (Fig. 4). Note that the BSG thickness is calculated by performing the cross-sectional measurement of SEM at the center of the sample

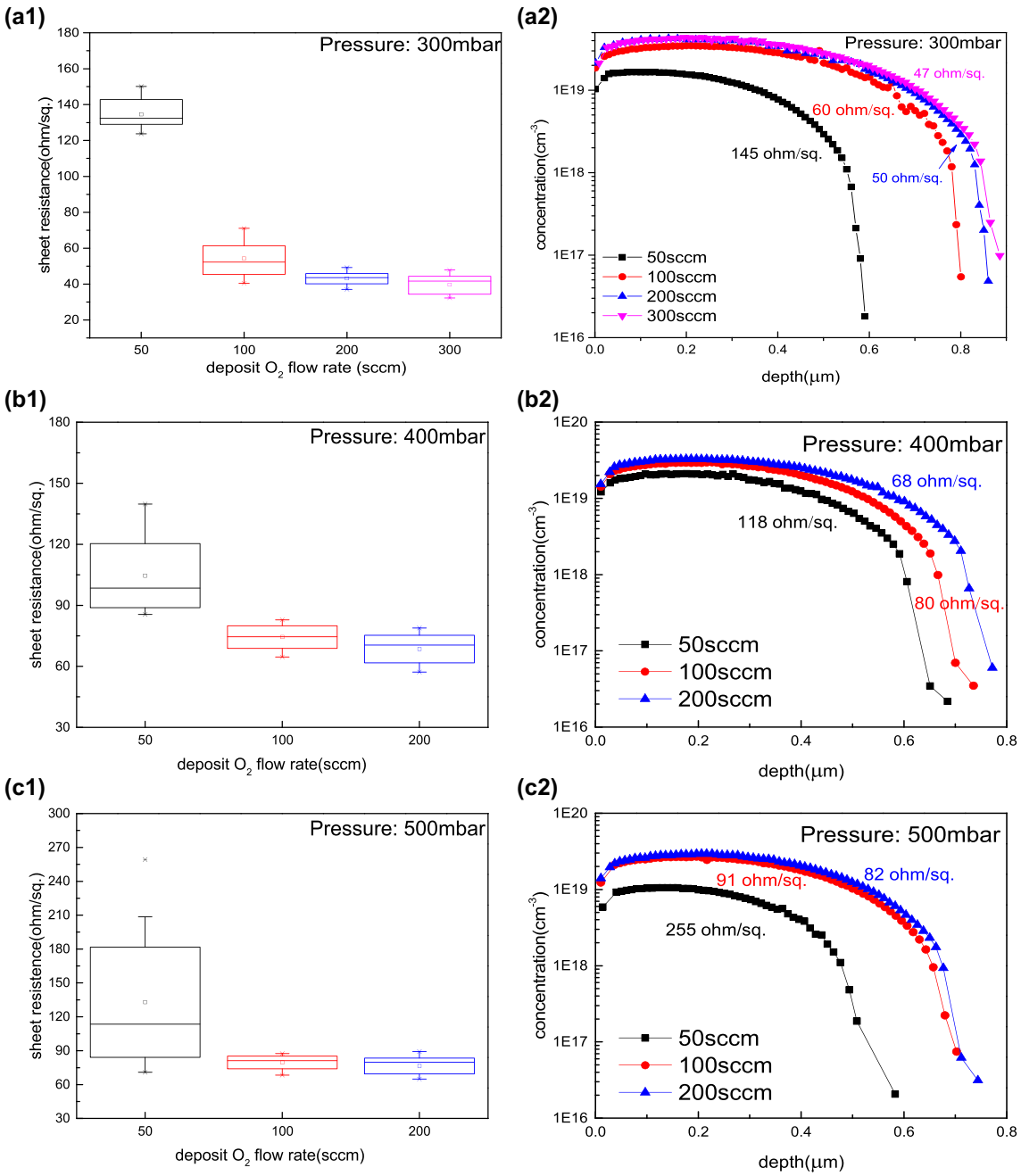

Fig. 3 The sheet resistance and doping profile for boron diffused samples prepared at different conditions: (a1) and (a2) 300 mbar; (b1) and (b2) 400 mbar; (c1) and (c2) 500 mbar

(Fig. 4a). It can be seen from Fig. 4b that the BSG thickness increases as the pre-deposition O_2 flow rate increases from 50 to 300 sccm with pressure of 300 mbar and the BSG thickness turns to be saturate when further increasing the O_2 flow rate, which is consistent with the change of sheet resistance. During the pre-deposition process, B atom is accumulated at the silicon surface and thicker BSG means higher B atom amount. In addition, the boron diffusion coefficient is dependent on the surface concentration and a higher surface concentration can lead to a higher boron diffusion coefficient [19], result in a deeper junction depth and a higher B doping concentration. However, the boron concentration turns to saturate as given higher O_2 flow rate, which shows a similar result to the depth profile of boron concentration based on different BBr_3 flow rates reported by Yvonne Schiele [20]. This phenomenon can be explained by the previous subject [21] that as growth of SiO_2 due to the oxidization of boron diffused layer or

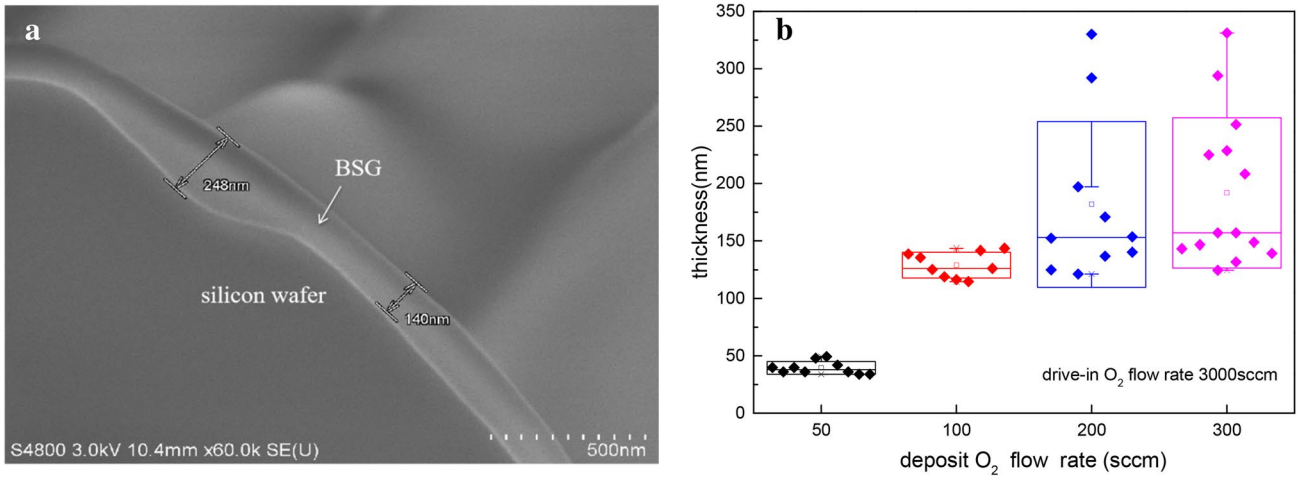

Fig. 4 **a** SEM Micrograph of BSG layer fabricated with deposit O_2 300sccm, drive-in O_2 3000sccm; (**b**) BSG thickness measured by SEM based on deposit O_2 flow rates (vacuum 300 mbar)

Si-B compound, the diffused amount of boron in BSG on the Si/SiO_2 surface is rapidly decreased.

Figure 5 shows the ECV profiles and sheet resistance based on vacuums with different O_2 flow rate and an increasing sheet resistance is obtained in Fig. 5a (pre-deposition O_2 flow rate 100sccm) and Fig. 5d (pre-deposition O_2 flow rate 200sccm). The unusual tendency obtained in Fig. 5c (deposit O_2 flow rate 50 sccm) should be attributed

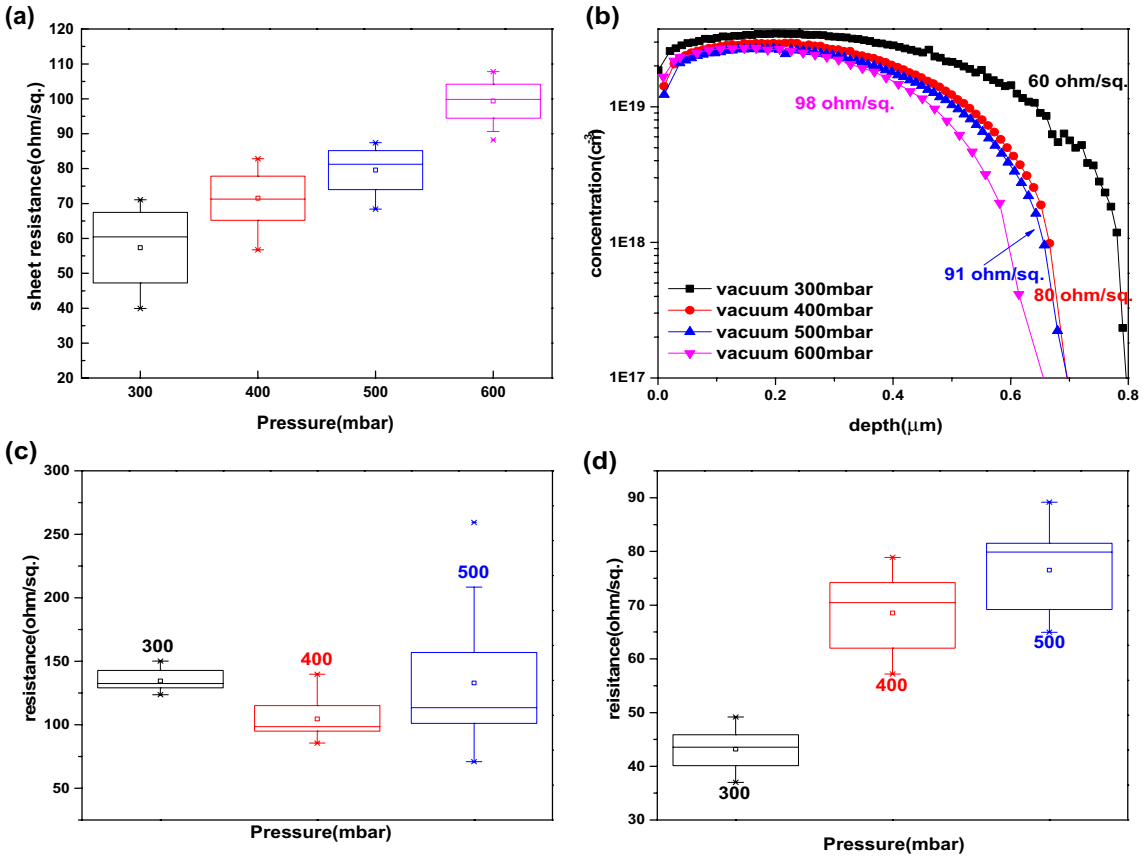

Fig. 5 Doping profiles and sheet resistance for boron diffused samples prepared at various pressures. **a**,**b** 100 sccm; (**c**) 50 sccm; (**d**) 200 sccm

to the worse sheet resistance uniformity. It can be seen from the ECV profiles that both the junction depth and the B atom concentration decreases as the pressure increases, which still cannot be understand.

The sheet resistance uniformity of the emitter is a very important factor in solar cell fabrication and the standard deviation (STDEV) is used to quantify the uniformity:

$$\mathrm{STDEV} = \sqrt{\frac{\sum_{i=1}^{n}\left(X_i - X\right)^2}{n-1}} \tag{1}$$

where X_i is each sheet resistance of the sample, X is the average value of the sheet resistance, and here n = 9 the number of tested points.

Table 2 shows the relationship between the STDEV of sheet resistance and the pre-deposition O_2 flow rate. It indicated that the diffusion uniformity between the samples is highly dependent on the O_2 flow rate, and the sheet resistance uniformity with the O_2 flow larger than 100 sccm is better than that with the O_2 flow of 50 sccm (the large STDEV, the worse uniformity), and the emitter formed with O_2 flow 200 sccm at pressure of 300 mbar shows the best uniformity. Moreover, the emitter formed in vacuum 300 mbar shows a better uniformity than others. As both the sheet resistance and BSG thickness are strongly dependent on the position of the silicon wafer [8, 22], it is understandable that the sheet resistance uniformity is related to the BSG thickness uniformity, however, the amount of active boron atoms is not fully dependent on the BSG layer thickness [23].

3.2 Drive-in O_2 flow rate

Figure 6 shows the sheet resistance and ECV profile as a function of drive-in O_2 flow rate at pressure of 300 mbar and 500 mbar, respectively. An increasing sheet resistance is observed as the drive-in O_2 flow rate increases from 0 to 3000 sccm at both pressure of 300 mbar and 500 mbar (Fig. 6a1, b1), which is contrary to the results of pre-deposition process. The ECV shown in Fig. 6a2, b2 indicate that, the B atom concentration decreases as the drive-in O_2 flow rate increases, result in an increasing sheet resistance. This phenomenon can be explained by considering the increase of diffusion enhancement ratio. As the diffusion enhancement ratio is linearly proportional to the oxidation rate [17], the higher drive-in O_2 flow rate shows a higher oxidation rate (can be obtained from Fig. 7), thus, more B atom diffuse into the silicon substrate, result in a lower B atom concentration. However, this means that a higher drive-in O_2 flow rate can also result in a deeper junction depth [24], which is not obvious in this paper. That unusual result should be due to the BSG removed process.

Table 3 shows the relationship between STDEV and the drive-in O_2 flow rate with different pressures. It can be seen that the best uniformity is obtained at pressure of 300 mbar no matter how much the drive-in O_2 flow rate is, besides, drive-in O_2 flow rate of 0sccm shows the best uniformity in every pressures.

3.3 Cell fabrication

The BSG film is very important in our TOPCon solar cell fabrication, for it can be a protect mask in wrap-around removed process. In order to remove the wrap-around of poly-silicon, the samples are immersed into 70 ℃ alkaline solution for 2 min and Fig. 8 shows the solar cell samples with/without wrap-around removed process. This section will investigate the relationship between the TOPCon cell properties and BSG thickness. All the samples are diffused in vacuum 300 mbar, with pre-deposition O_2 100 sccm, drive-in O_2 3000 sccm and various BSG thicknesses are realized by various times of single side HF solution treatment and Fig. 9f shows the BSG thicknesses as the function of HF treatment time.

The surface morphology based on BSG thickness with/without a wrap-around of poly-Si removed process has been shown in Fig. 9, and the surface morphology are measured after BSG removed process. It can be seen that after the wrap-around removed treatment, the surface of samples with 0 s and 135 s HF treatment are protected totally from the alkaline etching, while, the surface of samples with 180 s and 225 s HF treatment have been destroyed, result in a shallower junction depth (Fig. 10a). Besides, as the HF treatment time increases to 180 s, an obvious increase can be observed in reflectivity (Fig. 10b) between the wavelength 400 nm and 700 nm. It seems that a p + emitter with ~ 50 nm BSG can be survived completely from the wrap-around removed process in this paper. Figure 10c shows the EQE response based on the

Table 2 The uniformity of boron diffusion processed at different pre-deposition O_2 flow rate

Boron emitter uniformity (standard deviation)(ohm/sq.)	50 sccm	80 sccm	100 sccm	150 sccm	200 sccm
Pressure 300(mbar)	7–9	–	6–8	–	1–4
Pressure 400(mbar)	16–20	–	4–6	–	6–8
Pressure 500(mbar)	45–50	–	5–8	–	6–8
Pressure 600(mbar)	–	9–11	–	6–8	5–10

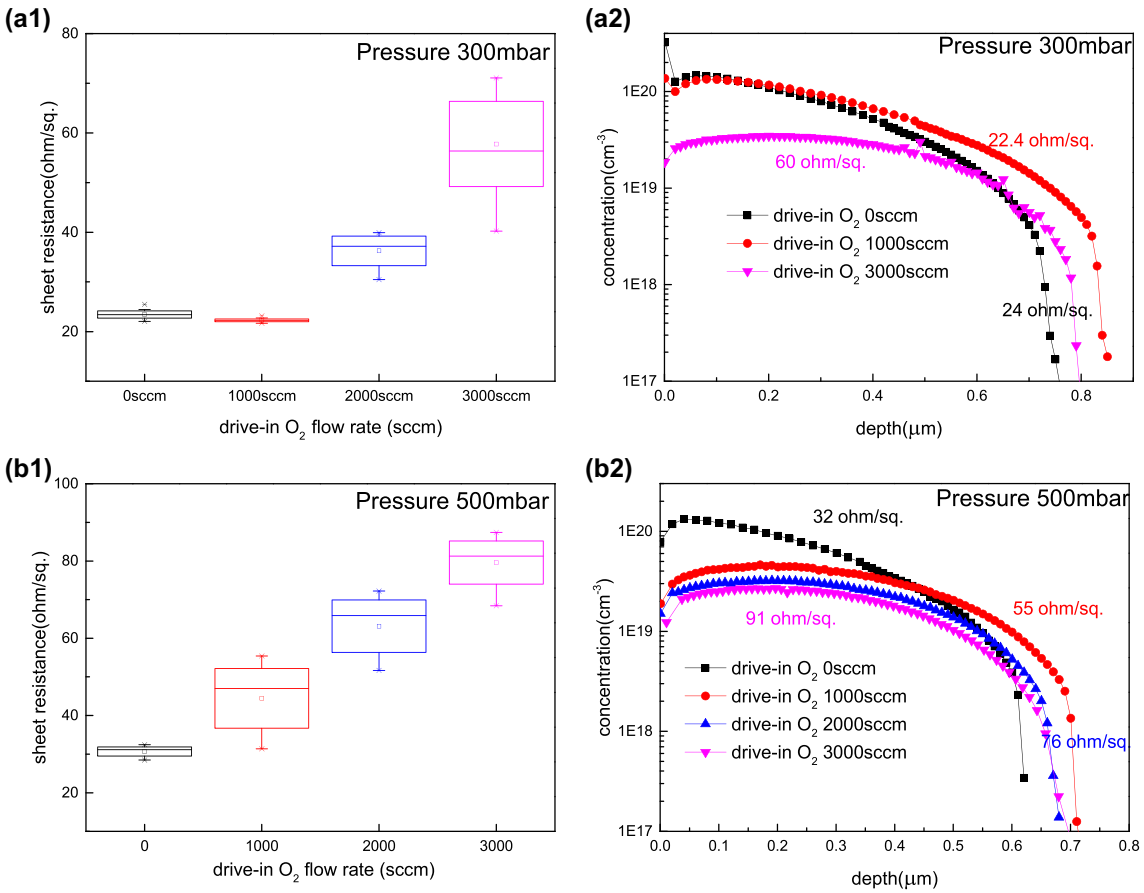

Fig. 6 The sheet resistance and doping profile for boron diffused samples prepared with different drive-in O_2 flow rate: (a1) and (a2) Pressure 300 mbar; (b1) and (b2) Pressure 500 mbar

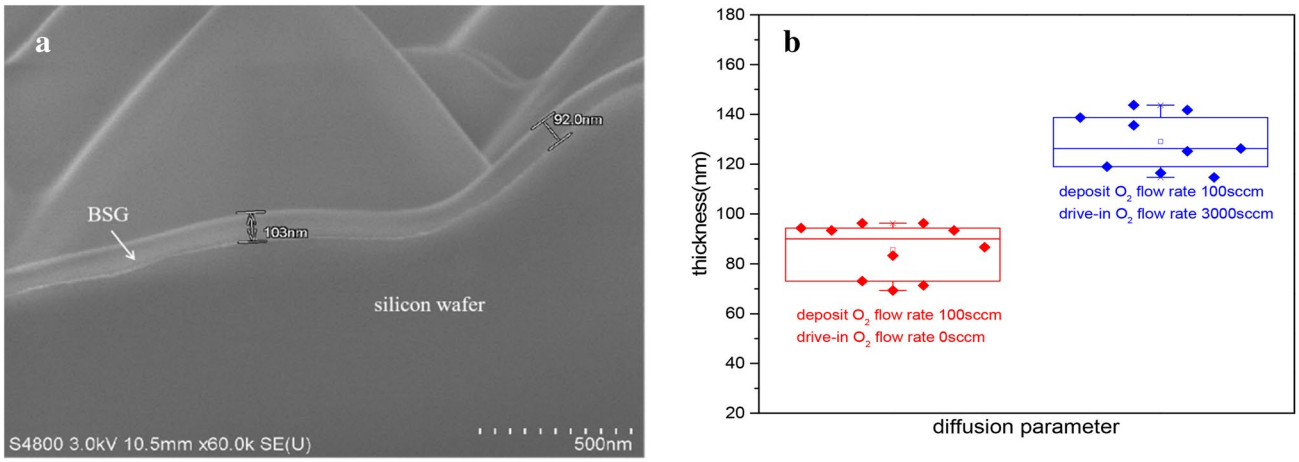

Fig. 7 **a** SEM Micrograph of BSG layer fabricated with pre-deposition O_2 100sccm, drive-in O_2 0sccm; (**b**)BSG thickness measured by SEM based on O_2 diffusion parameter (vacuum 300 mbar)

BSG thickness between wavelength 300–700 nm and the blue response increases as the HF treatment time increases from 0 to 135 s. The change of the EQE response of the sample with 180 s HF treatment should attribute to the change of B doping profile and reflectivity. In addition, due to the increases of sheet resistance and the destroy of surface, the contact resistivity of the front side increases from 0.9 ± 0.2 mohm·cm^2 to 2.6 ± 1 mohm·cm^2.

Table 3 Boron emitter uniformity depend on the drive-in O_2 flow rate

Boron emitter uniformity (STDEV) (ohm/sq.)	O_2 0 sccm	O_2 1000 sccm	O_2 2000 sccm	O_2 3000 sccm
Pressure 300(mbar)	0–1	0–1	3–4	4–5
Pressure 400(mbar)	0–1	3–5	7–8	5–7
Pressure 500(mbar)	1–2	7–9	6–8	5–7

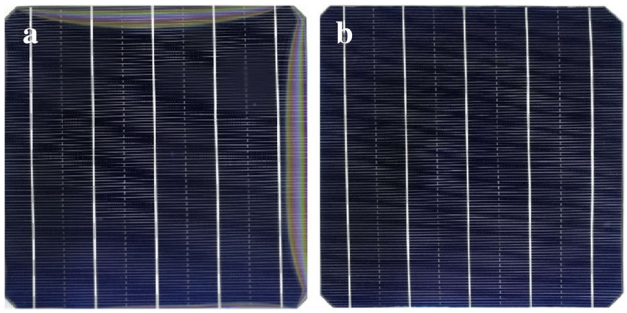

Fig. 8 TOPCon solar cell sample (**a**) with wrap-around of poly-Si (**b**) wrap-around of poly-Si removed

Based on the results above, an optimized p + emitter is prepared for TOPCon solar cells using boron trichloride, with 70–90 ohm/sq. sheet resistance and ~ 100 nm BSG thickness. The obtained TOPCon solar cells exhibit a high efficiency of 22.14%, with V_{oc} of 683.4 mV, J_{sc} of 39.53 mA/cm^2, FF of 81.96% (as shown in Fig. 10d). Further works are still needed to further improve the output of cells, for example, optimization of light trapping, improving the surface passivation of the front emitter, and so on. And works is underway to quantify and explore the potential benefits compared to the more developed and widely applied other solar cell structures.

4 Conclusion

We developed varies pre-deposition and drive-in O_2 flow rate doping process using BCl_3 as doping source in different vacuums. A reduction of sheet resistance is observed as the pre-deposition O_2 flow rate increases from 50 to 300 sccm, and an increasing of sheet resistance is observed as the drive-in O_2 flow rate increases from 0 to 3000 sccm.

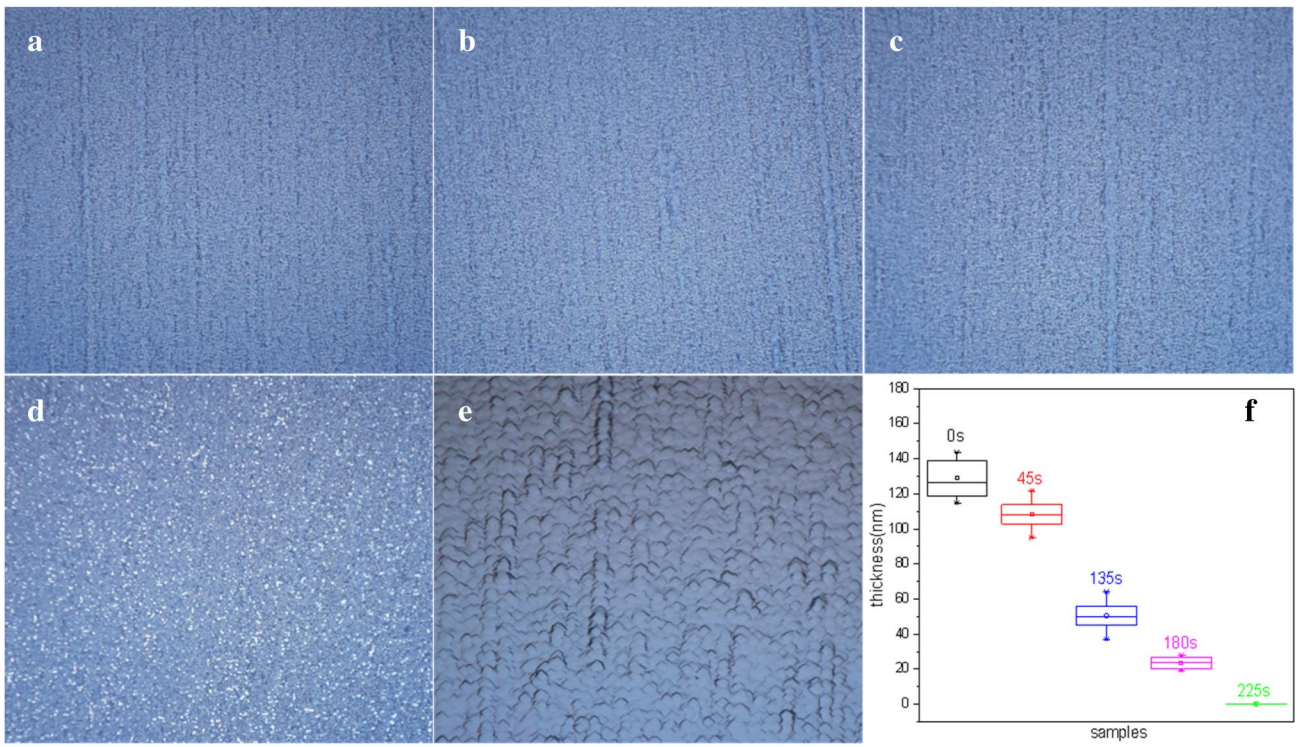

Fig. 9 surface morphology of samples (**a**) 0 s HF treatment without wrap-around removed treatment; (**b**) 0 s HF treatment (**c**) 135 s HF treatment (**d**) 180 s HF treatment (**e**) 225 s HF treatment (no BSG) with wrap-around removed treatment

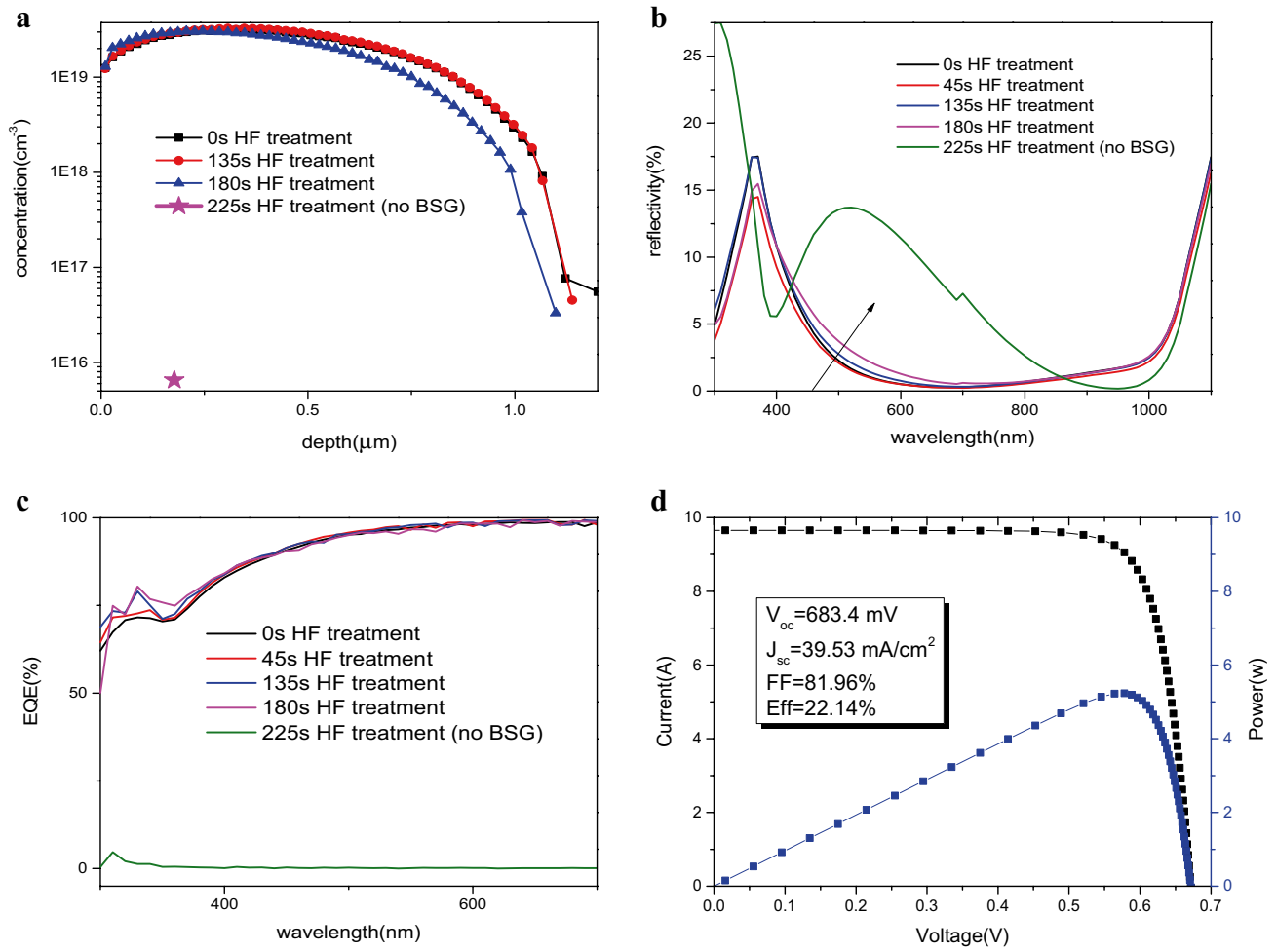

Fig. 10 **a** boron doping profile and (**b**) Reflectivity and (**c**) EQE of samples with various BSG thickness after wrap-around removed treatment (**d**) Light I–V curve of champion TOPCon cell

In addition, the emitter formed in vacuum 300 mbar shows a better uniformity than others. Both the pre-deposition O_2 and drive-in O_2 flow rate play important roles in BSG thickness, and the TOPCon solar cells fabricated with various BSG thickness has been investigated and compared. The result shows that a p + emitter with a thick BSG thickness(> 50 nm) is necessary in industrial TOPCon solar cell fabrication process due to the wrap-around of poly-Si removed process. Finally, based on the optimized p + emitter formed by thermal diffusion of BCl_3 (~ 100 nm thickness BSG, 70–90 ohm/sq. sheet resistance), high efficiency 22.14% n-type TOPCon on 244.32 cm^2 Cz is fabrication with a V_{oc} of 683.4 mV, J_{sc} of 39.53 mA/cm^2 and FF of 81.96%.

Acknowledgements This work was supported by the National Key Research and Development Program of China (2018YFB1500500, 2018YFB1500200), National Natural Science Foundation of China (NSFC, Grant Nos. 51602340, 51702355), Natural Science Foundation of Beijing Municipality (4192064) and JKW Project 31512060106.

References

1. F. Feldmann, M. Bivour, C. Reichel, et al. A passivated rear contact for high-efficiency n-type silicon solar cells enabling high VocS and FF>82%. in *Presented at the 28th European PV Solar Energy Conference and Exhibition* (2013)
2. Di Yan, A. Cuevas, S.P. Phang, 23% efficient p-type crystalline silicon solar cells with hole-selective passivating contacts based on physical vapor deposition of doped silicon films. Appl. Phys. Lett. **113**(6), 061603 (2018)
3. K. Tao, Q. Li, C. Hou, Application of a-Si/μc-Si hybrid layer in tunnel oxide passivated contact n-type silicon solar cells. Sol. Energy **144**, 735–739 (2017)
4. F. Feldmann, C. Reichel, R. Müller et al., The application of poly-Si/SiO x contacts as passivated top/rear contacts in Si solar cells. Sol. Energy Mater. Sol. Cells **159**, 265–271 (2017)
5. M.K. Stodolny, M. Lenes, Y. Wu et al., n-Type polysilicon passivating contact for industrial bifacial n-type solar cells. Sol. Energy Mater. Sol. Cells **158**, 24–28 (2016)
6. Y. Zhou, Ke Tao, A. Liu et al., The impacts of LPCVD wrap-around on the performance of n-type tunnel oxide passivated contact c-Si solar cell. Curr. Appl. Phys. **20**(7), 911–916 (2020)

7. A. Teppe, C. Gong, K. Zhao, Progress in the industrial evaluation of the mc-Si PERCT technology based on boron diffusion. Energy Procedia **77**, 208–214 (2015)
8. R. Cabal, Y. Veschetti, V. Sanzone et al., Industrial process leading to 19.8% on N-type Cz silicon. Energy Procedia **33**, 11–17 (2013)
9. J. Armand, C. Oliver, F. Martinez, Modeling of the boron emitter formation process from BCl_3 diffusion for N-type silicon solar cells processing. Adv Materials Res **324**, 261–264 (2011)
10. R. J. Kriegler, Y. C. Cheng, D. R. Colton, The effect of HCI and on the thermal oxidation of silicon. J. EIectrochem. Soc. Solid State Sci. Technol., pp 388–392 (1972)
11. R. Amaro e Silva, Empirical optimization and implementationof a boron emitter on n-type silicon solar cells using a BBr3 liquid source. Mestrado Integrado em Engenharia da Energia e do Ambiente (2014)
12. A.M. Lin, R.W. Dutton, D.A. Antoniadis, The lateral effect of oxidation on boron diffusion in ⟨100⟩ silicon. Appl. Phys. Lett. **35**(10), 799–801 (1979)
13. A. Miin-Ron Lin, D. A. Antoniadis, R. W. Dutton, The oxidation rate dependence of oxidation-enhanced diffusion of boron and phosphorus in silicon (1981)
14. M. Miyake, Oxidation-enhanced diffusion of ion-implanted boron in heavily phosphorus-doped silicon. J. Appl. Phys. **58**(2), 711–715 (1985)
15. K. Taniguchi, K. Kurosawa, M. Kashiwagi, Oxidation enhanced diffusion of boron and phosphorus in (100) silicon. J. EIectrochem. Soc. (1980)
16. D.A. Antoniadis, I. Moskowitz, Diffusion of substitutional impurities in silicon at short oxidation times: an insight into point defect kinetics. J. Appl. Phys. **53**(10), 6788–6796 (1982)
17. A. Miin-Ron Lin, D.A. Antoniadis, R.W. Dutton, The oxidation rate dependence of oxidation-enhanced diffusion of boron and phosphorus in silicon. J. Electrochem. Soc. **128**(5), 1131–1137 (1981)
18. W. Kern, D.A. Puotinen, Cleaning solutions based on hydrogen peroxide for use in silicon semiconductor technology. RCA Rev. **31**, 187–206 (1970)
19. P.M. Prasad, V.P. Sundarsingh, Diffusion of boron into silicon from doped oxide source. Microelectron. J. **11**(6), 21–24 (1980)
20. Y. Schiele, S. Fahr, S. Joos, et al. Study on boron emitter formation by BBR_3 diffusion for n-type Si solar cell applications. in *28th European Photovoltaic Solar Energy Conference and Exhibition* (2013)
21. E. Arai, H. Nakamura, Y. Terunuma, Interface reactions of B_2O_3-Si system and boron diffusion into silicon. J. Electrochem. Sac **120**(7), 980–987 (1973)
22. M.A. Kessler, T. Ohrdes, B. Wolpensinger et al., Charge carrier lifetime degradation in Cz silicon through the formation of a boron-rich layer during BBr 3diffusion processes. Semiconductor Sci. Technol. **25**(5), 055001 (2010)
23. V. S. R. Monna, J. Diaz, Y. Veschetti, Influence of the BCl3 diffusion process homogeneity on the surface passivation of n-type PERT solar cells. in *6th International Conference on Silicon Photovoltaics* (2016)
24. J. Armand, C. Oliver, B. Semmache, Modelling and analysis of the emitter boron process under BCL_3 and O_2 for industrial silicon solar cells applications. in *26th European Photovoltaic Solar Energy Conference and Exhibition*, pp. 1309–1312